Reliability Enhancement of Synchrophasor-Based DTR system considering N-1 contingency for PMU placement

Bilkisu Jimada-Ojuolape
School of Electrical and Electronic Engineering
Universiti Sains Malaysia
Penang, Malaysia
Department of Electrical and Computer Engineering
Kwara State University, Nigeria
0000-0001-8592-8438

2021 IEEE International Future Energy Electronics Conference (IFEEC) | 978-1-6654-3448-5/21/$31.00 ©2021 IEEE | DOI: 10.1109/IFEEC53238.2021.9662031

***Abstract*—The cyber power network has become more intelligent and efficient because of the integration of information and communication technology (ICT) infrastructure. By combining intelligent infrastructure such as phasor measurement units (PMUs), smart sensors, and other two-way communication and monitoring capabilities, this enhances reliability and sustainability. They do, however, have some disadvantages, such as component and communication network failures, as well as cyber breaches, which might compromise the existing network's reliability. Dynamic Thermal Rating (DTR) systems which is a smart grid technology, improves existing line ratings by allowing them to be increased based on several parameters without violating line safety requirements. Thus, this paper presents a DTR system that uses PMUs to implement Wide Area Monitoring (WAM) functions and investigates the impact of PMU failures and line outages on cyber-physical network reliability. The study uses a Monte Carlo simulation-based method to carry out the investigation on the IEEE RTS while considering the impacts of seven and thirteen PMUs. The test network is modified to emphasize the benefits of ICTs and the findings show that using PMUs enhances reliability greatly. While the use of seven PMUs offers reliability improvement by 53.15%, the use of 13 PMUs offers more significant improvement (by 95.79%) because a single line outage will not affect network observability.**

Keywords— Cyber-Physical Systems, Dynamic Thermal Rating, Phasor Measurement Units, Power System Reliability, Smart Grid

I. INTRODUCTION

The application of ICT capabilities to cyber-physical power networks has a significant impact on power system reliability. These ICT capabilities can be used to enhance the power network with the aid of certain technologies such as demand side management (DSM) techniques which is used to educate and inspire customers to change their energy consumption patterns to avoid using energy during peak hours when network demands are high and market prices are high, compromising network reliability [1]–[3]. Distributed Energy Resources (DER) is another avenue to utilize ICT features on the power network. These DERs include hydro energy, photovoltaics, wind, distributed generation, energy storage systems, and electric vehicles [4]–[7]. However, there are looming threats such as component failures, environmental consequences, and cyber-attacks [8], [9].

Thermal limitations are the factors that determine the highest temperature at which the lines can operate safely and reliably given their current carrying capacity. Transmission line thermal rating methods are classed as Static Thermal Ratings (STR) or Dynamic Thermal Ratings (DTR). On conventional power networks, STRs are conservative values that are programmed and routinely used based on certain assumptions. DTR, on the other hand, is a variable quantity and another way of deploying ICTs on power networks. DTR values can be calculated directly by measuring line characteristics like voltage and temperature, conductor slope, ground clearance, and line loading, or indirectly by using variables like projected or measured weather information like wind speed and direction, solar radiation, precipitation, and ambient temperature [10]. To determine DTR values, these measurements are combined with standards such as the CIGRE and IEEE 738. According to studies, DTR has the ability to increase line ratings by up to 30%, and in windy places, this value might be as high as 50% [11]–[13]. DTR reduces carbon emissions, reduces line congestion, and lowers system operators' costs. It allows them to improve electricity networks without having to invest in costly infrastructure upgrades, and it generally improves operations, increasing network reliability [10]. Unwanted system disruptions could arise because the DTR system supports uprating the lines and allowing them to operate closer to their actual limits. If one line fails, thermal overloading may develop, resulting in cascading failures on the network [8], [10]. DTR installation has unquestionably proven to be cost-effective and reliable. The variable thermal expansion, on the other hand, creates additional mechanical stress on the lines, which might cause them to age more quickly.

Phasor measurement units (PMUs) are Intelligent electronic devices (IEDs) that estimate synchrophasors of which the input parameters are measured directly from the lines through instrument transformers and reports same to the phasor data concentrator (PDC). As lines are operated closer to their thermal limitations, sag clearance breaches can occur when the transmission line is heavily loaded or when a single line is down, resulting in cascaded line interruptions and faster network ageing. PMUs can help to decrease this risk since they provide direct measurement of line parameters, which generally makes DTR calculations more accurate. To achieve full network observability, only a small number of PMUs are deployed on the network and this is the subject of some studies [14]–[17]. By sampling bus voltages and currents, the PMUs

978-1-6654-3448-5/21/$31.00 ©2021 IEEE

Authorized licensed use limited to: University of Durham. Downloaded on January 06,2022 at 14:00:51 UTC from IEEE Xplore. Restrictions apply.

evaluate the status of the entire network and offer data to aid in the calculation of the new uprated line capacity value. A PMU can estimate the voltage at the opposite end of the line by sampling current phasors. The PMUs estimate the state of the entire network by sampling bus voltages and currents and provides the information to aid the calculation of the new uprated value of line capacity. The sampling of current phasors allows a PMU to estimate the voltage at the other end of the line. This feature allows a single PMU to monitor the bus it is installed on as well as all other adjacent buses [18], [19].

Several papers have been published that discuss the reliability of DTR systems and their impact on system-wide reliability [11], [20]–[22]. DTR systems, as previously said, operate through the integration of ICT systems, however, very few studies have examined the impact of the ICT system on system-wide reliability more so, studies that implement DTR using PMUs. Studies [23]–[25] perform DTR assessment with the use of PMUs but without considering the impact of cyber sub system failures.

The proposed concept in this study is a cyber-physical network that employs PMUs for WAM applications to implement DTR features on the network. The information from synchrophasor data obtained from PMUs deployed on strategic buses throughout the network is used to determine dynamic line ratings. Thus, the main objective of this study is to investigate the impact of PMU failures and line outages on cyber-physical network reliability. This is done check the extent of reliability improvement when thirteen (13) PMUs are considered compared with when seven (7) PMUs are deployed on the cyber-physical network.

The remainder of the paper is structured as follows. Section II describes the proposed method employed to carry out the reliability evaluation and section III describes the modelling scenarios as well as the results obtained. In section IV, some avenues for future work are highlighted while the paper is concluded in section V.

II. METHODOLOGY

A. PMU placement and Network observability

In this study, 13 PMUs are employed to fully observe the network considering N-1 contingency. This implies that the outage of a single line will not impact PMU observability negatively if the PMUs are available i.e., in up state. Previous studies have proposed the use of 7 PMUs which will also fully observe the network but in this case the N-1 contingency principle is not considered, and a single line outage could affect network observability severely. The first observability rule is that a PMU placed on a bus will observe itself i.e., that bus and all other adjacent buses, otherwise the bus is unobservable. This is formulated as (1). The second rule is that if both buses at the ends of a particular line are observable then the line is also deemed observable, otherwise, the branch is unobservable [26]. This is formulated as (2).

$$BusObs(B) = \begin{cases} 1, & if\ A_{PMU}^{B} = 1 \quad B \in B_{PMU} \\ & if\ A_{PMU}^{AB} * A_{L}^{AL} = 1 \quad AB \in AB_{PMU} \\ 0, & otherwise \quad \forall B \end{cases} \tag{1}$$

$$BrObs(L) = \begin{cases} 1, & if\ BusObs(B) * BusObs(AB) = 1 \\ 0, & otherwise \end{cases}, \quad \forall L \tag{2}$$

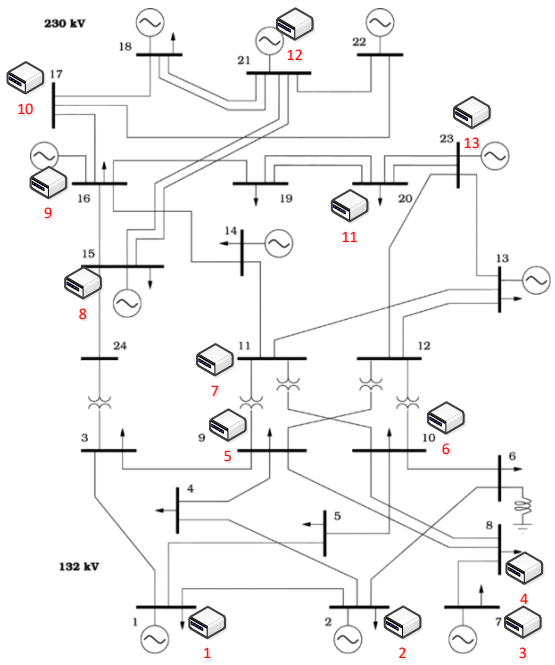


Fig. 1. Modified CPTS showing placement of 13 PMUs

The PMUs are placed on buses 1, 2, 7, 8, 9, 10, 11, 15, 16, 17, 20, 21 and 23 on the network [17]. This can be seen in *Fig. 1*. Thus, PMU 1 on bus 1 observes buses 1, 2, 3 and 5.

B. DTR model

The instrument transformers (Current Transformers (CT) and Potential Transformers (PT) take readings from the lines and send them to the PMUs to calculate the 3-phase current and voltage synchrophasors. Each PMU requires three functional CTs and PTs to obtain the required measurements. When all the ICT components are operational, the values of the calculated synchrophasors are regarded available, and the network is observable. Otherwise, they are unavailable, making the buses and lines adjacent to them unobservable. The DTR model is shown in *Fig. 2*.

The availability of the DTR system is then formulated by computing the availabilities of each of the ICT components. Once all required components are available, then DTR values can be calculated and deployed on the lines. The indirect technique is used to determine the DTR value of the line based on the IEEE 738 standard, while incorporating ACSR "Drake"

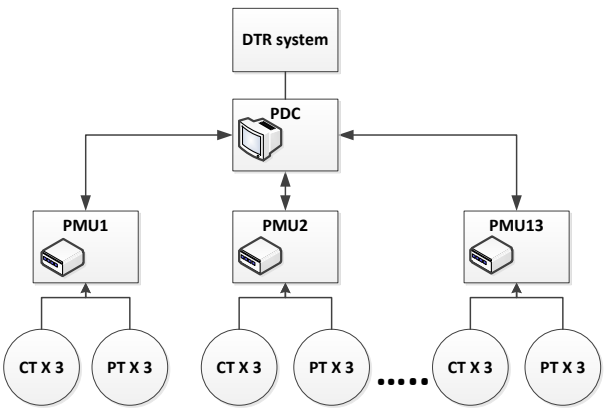


Fig. 2. DTR model

Authorized licensed use limited to: University of Durham. Downloaded on January 06,2022 at 14:00:51 UTC from IEEE Xplore. Restrictions apply.

and "Lapwing" conductor properties shown in Table 1 and meteorological data from the Center for Environmental Data Analysis (CEDA) archive [10], [27], [28]. This is formulated as (3).

$$I = \sqrt{\frac{q_c(\theta, T_a, V_w, \varphi) + q_r(\theta, T_a) - q_s}{R(\theta)}} \quad (3)$$

where convection heat loss = q_c, radiated heat loss = q_r, solar radiation heat gain = q_s and joule heat gain = $I^2R(\theta)$. I is the ampacity and R(θ) is the conductor resistance.

TABLE 1 LINE PROPERTIES

Conductor (ACSR)	Base Volt (kV)	Diameter (mm)	Resistance at 75°C (Ω/m)	Resistance at 25°C (Ω/m)	STR (MVA)
Drake (26/7)	138	28.1	0.00008688	0.00007283	175
Lapwing (45/7)	230	38.2	0.00004440 6	0.00003667 3	500

C. Simulation Algorithm

Step 1) The DTR values are pre-calculated based on the weather and transmission line physical properties at an hourly rate for a simulation year and loaded into the simulation.

Step 2) The statuses of all network components including the ICT components (PMUs, CTs, and PTs) and transmission lines are sampled at an hourly rate for a simulation year to determine which elements are functional.

Step 3) Network observability is determined based on the availability of the ICT components.

a. If the lines are observable, DTR ratings are applied for those lines which are considered available.

b. Otherwise, STR values are applied for the unobservable portions of the network.

Step 4) The DCOPF is executed to determine the power flows after which, the indices are updated.

Step 5) The previous steps are iterated until convergence occurs.

The proposed algorithm described above is shown in Fig. 3.

D. Power flow formulation

The load curtailment problem is formulated as (4).

$$\min f_{DCOPF}(P_f) = \left(\sum_{i \in LB} C_d\right) \quad (4)$$

subject to

$$\sum_{g \in GB} PG_g + \sum_{i \in LB} C_i = \sum_{i \in LB} PD_i \quad (4a)$$

$$PG_g^{min} \le PG_g \le PG_g^{max}, \quad \forall g \in GB \quad (4b)$$

$$0 \le C_d \le PD_d, \quad \forall d \in LB \quad (4c)$$

$$|PF_l| \le PF_l^{max} = \begin{cases} PF_l^{DTR}, & \forall l \in OL \\ PF_l^{STR}, & \forall l \in UL \end{cases}$$

In (4a) the power balance requirement on each bus is described, while generation and load curtailment constraints

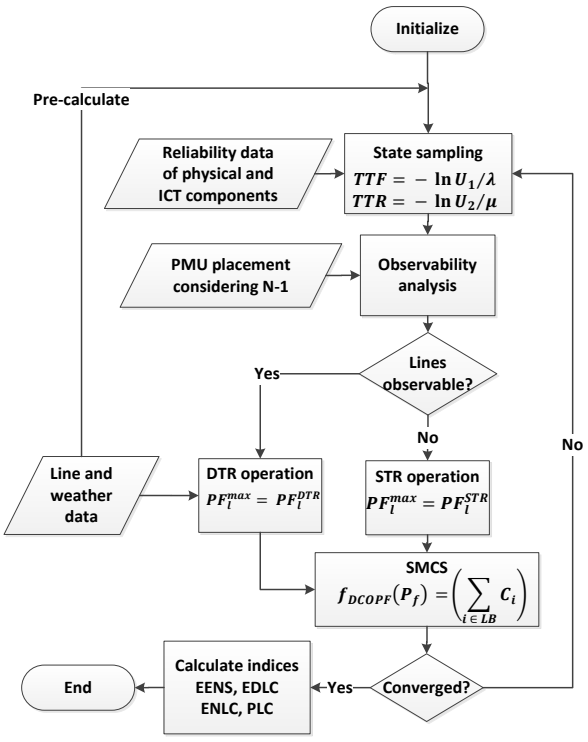


Fig. 3. Simulation algorithm

are considered in (4b) and (4c). (4d) is the maximum line rating for each line which is either equal to the DTR value for all observable lines (OL) or STR for all unobservable lines (UL).

The following reliability indices are calculated to assess the impact of ICT failures on the modified network's reliability based on different numbers of PMUs [29], [30].

1) Probability of Load Curtailment (PLC):

$$PLC = \sum_{i \in S} p_i \quad (5)$$

where pi is the system state probability of load curtailment while S is a set of all system states.

2) Expected Energy Not Supplied (EENS): it is the ratio of undelivered energy to total energy demand for the same analysis period.

$$EENS = \sum_{i \in S} 8760\, C_i P_i \quad (MWh/yr) \quad (6)$$

where *i* is the system state at a particular time, S is a set of all system states, C_i is the load curtailment of system state *i* and P_i is the probability of system state i

3) Expected Number of Load Curtailment (ENLC): this index represents the summation of the load curtailment occurrences in a system state.

$$ENLC = \sum_{i \in S} \left(P_i \sum_{k \in N} \lambda_k\right) \quad (occ./yr) \quad (7)$$

(4d)

where λ_k is the rate of departure of a system component with respect to system state *i* while *N* is the set of all possible departure rates in that system state.

Authorized licensed use limited to: University of Durham. Downloaded on January 06,2022 at 14:00:51 UTC from IEEE Xplore. Restrictions apply.

4) Expected Duration of Load Curtailments (EDLC): this index represents the mean duration for the period when the network cannot meet the load demand in a sample year.

$$EDLC = PLC \times 8760 \quad (hr/yr) \qquad (8)$$

III. Modelling Scenarios, Results, and Discussion

A modified IEEE RTS-79 is employed to implement the proposed approach as previously mentioned. To ensure that the lines are fully utilized, the generation capacity and load demand are boosted up to three times the rated specification. This change emphasizes the advantages of uprating transmission lines. The physical network's reliability data can be found in [31] while the ICT components reliability data is culled from [19]. Three different scenarios are simulated to check the impact of PMU failures on the synchrophasor-based CPS.

Scenario 1: This scenario models the impacts of only physical network failures while assuming that the lines are operated on the STR values. This implies that DTR is assumed not available on the network.

Scenario 2: DTR is implemented in this scenario and the impacts of 7 PMUs on the network are modelled. The PMUs are placed on buses 2, 3, 8, 10, 16, 21, 23.

Scenario 3: This scenario also implements DTR but checks the impact of 13 PMUs on the network. This last scenario models the reliability improvement considering additional PMUs and N-1 contingency.

The network is assessed based on the proposed method described in section 2 and while considering the modelling scenarios described above. The results of the simulation are presented in *Table 2*.

Table 2 Assessment results

Sc.	No of PMUs	PLC	EENS (MWh/yr)	EDLC (hr/yr)	ENLC (Occ./yr)
1	0	0.027	153100	235	13
2	7	0.062	71735 (53.15%)	542	85
3	13	0.009	6446 (95.79%)	76	12

In scenario 1, where it is assumed that there are no PMUs and ICT components on the network and the network is operated solely on STR, it can be observed that the total load curtailed has the highest value. This is expected as the network demand is much more than it can supply based on the current system conditions of the network in which the total capacity has been increased to showcase DTR benefits. EDLC and ENLC are somewhat moderate because only transmission line outages provoke load shedding which is quite minimal as N-1 contingency is generally considered for transmission line outage.

In scenario 2, is assumed that seven PMUs are deployed on the network. Seven PMUs are enough to fully observe the network as a single PMU can observe up to two buses as is the case of bus 1 observed by PMUs 1 and 2 as shown in Fig. 4. Although this number of PMUs is sufficient to achieve full network observability, not so many spare measurements are available to provide redundancy. This simply implies that the outage of a single PMU will cause a total loss of observability for some portions of the network. In this case 15 of the 24 buses are observed by a single PMU so those buses stand a higher chance of losing observability when a single PMU is out. For example, if PMU 1 is down then bus 2 and 4 become totally unobservable since no other PMU's observe those buses. Another event that can lead to loss of observability is the outage of transmission lines since adjacent bus observability depends on line availability. This implies that when an adjoining line is down, observability is lost to connecting buses despite the availability of the PMUs. An example of this event is the case of PMU 1 observing adjacent bus 4 via $L_{2\text{-}4}$. If $L_{2\text{-}4}$ is on outage, then bus 4 cannot be observed even if PMU 1 is available. Consequently, total loss of observability implies that those unobservable portions cannot be upgraded to DTR values which in turn means load curtailment will be incurred. This can be observed on Table 2 where EENS value is 71735MWh/yr. However, compared to scenario 1 this EENS value is significantly improved by 53.15%. Curiously, EDLC and ENLC values in which network components contribute to load loss are much higher in this scenario than in scenario 1. This is because in scenario 1 only transmission line outages contribute to load curtailment whereas in scenario 2 both transmission line and PMU outages will provoke load loss. Due to this, PLC is also higher in this scenario than in scenario 1.

In scenario 3, it is assumed that thirteen PMUs are placed on the network as shown in Fig. 1. Just like the use of seven PMUs, the placement of thirteen PMUs means that the network is completely observable, but redundancy is provided by the addition of 6 more PMUs. In this scenario, spare measurements are available to cushion the effects of single PMU and single line outage contrary to scenario 2. For example, bus 8 can be observed by up to four PMUs (3, 4, 5, 6), this means that the loss of 1 or 2 or even 3 of those PMUs or adjoining lines will not cause a loss of observability for that

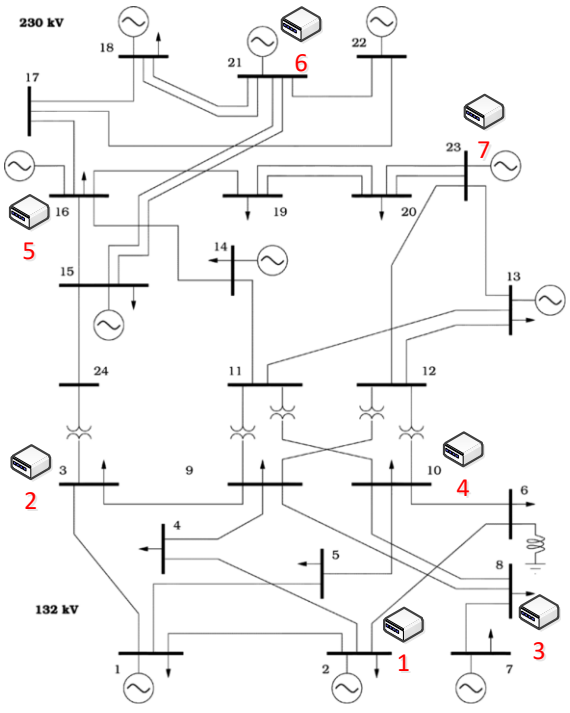


Fig. 4 PMU placement showing 7 PMUs

Authorized licensed use limited to: University of Durham. Downloaded on January 06,2022 at 14:00:51 UTC from IEEE Xplore. Restrictions apply.

bus. This means that for this bus there is only a 6.25% chance of total loss of observability. Throughout the network, only bus 24 is observed by a single PMU, all other buses are observed by at least two PMUs meaning there is a 25% chance or less of total loss of observability. This significantly reduces the total amount of load curtailed as can be observed by the results on Table 2 where EENS is 95.79% less than scenario 1 and 91.01% less than scenario 2 signifying an improvement in total network reliability. Interestingly, even the duration and number of load curtailment are significantly lower in this scenario. This is because the probability of load curtailment has significantly reduced due to the increased number of PMUs placed on the network. Ultimately this means that much fewer events of load curtailment are experienced which also translates to a much lower EENS. It can be seen that ENLC in this scenario is quite similar to the value in scenario 1 but in this scenario the number of load curtailed causes a shorter duration of load curtailment again because of the increased number of PMUs that dampen this impact.

IV. Future Work

An important limitation of this study is that the impacts of functional PMU failures where the PMU sends bad data to the PDC are not considered. Also, the reliability of the communication medium in which the PMUs and the PDCs utilize are also not considered in this study. These are important directions for further studies because these factors will also have specific effects on network reliability.

V. Conclusion

This research proposed a way for emulating WAM capabilities on a DTR system using PMUs, CTs, and PTs. The failures of these components are taken into account to demonstrate their impact on overall system reliability. Three cases are investigated, and the findings show that the implementation of DTR on the network provides a boost in overall system-wide reliability. Although seven PMUs are sufficient for total network observability, the loss of a single PMU or transmission line greatly increases load curtailment, nonetheless reliability is improved by 53.15%. The implementation of thirteen PMUs is then investigated and this scenario offers far greater improvements in reliability as can be observed in the results presented in Table 2. Less load shedding will be provoked when thirteen PMUs are used on the network since there are more redundant measurements to support single PMU and single line outages, and thus accounting for the N-1 principle. This is why the EDLC and ENLC results are much lower in scenario 3 than scenario 2. Overall, the results demonstrate a more significant improvement in reliability when thirteen PMUs are utilized by 95.79%.

References

[1] W. C. Khoo, J. Teh, and C.-M. Lai, “Integration of Wind and Demand Response for Optimum Generation Reliability, Cost and Carbon Emission,” IEEE Access, vol. 8, pp. 183606–183618, 2020.

[2] W. K. Khoo, J. Teh, and C. Lai, “Demand Response and Dynamic Line Ratings for Optimum Power Network Reliability and Ageing,” IEEE Access, vol. 8, pp. 175319–175328, 2020.

[3] M. K. Metwaly and J. Teh, “Probabilistic Peak Demand Matching by Battery Energy Storage Alongside Dynamic Thermal Ratings and Demand Response for Enhanced Network Reliability,” IEEE Access, vol. 8, pp. 181547–181559, 2020.

[4] F. Mohamad, J. Teh, and C. M. Lai, “Optimum allocation of battery energy storage systems for power grid enhanced with solar energy,” Energy, vol. 223, p. 120105, 2021.

[5] F. Mohamad, J. Teh, and H. Abunima, “Multi-Objective Optimization of Solar/Wind Penetration in Power Generation Systems,” IEEE Access, vol. 7, pp. 169094–169106, 2019.

[6] M. K. Metwaly and J. Teh, “Optimum Network Ageing and Battery Sizing for Improved Wind Penetration and Reliability,” IEEE Access, vol. 8, pp. 118603–118611, 2020.

[7] J. Teh and C. M. Lai, “Reliability impacts of the dynamic thermal rating and battery energy storage systems on wind-integrated power networks,” Sustain. Energy, Grids Networks, vol. 20, p. 100268, 2019.

[8] B. Jimada-ojuolape and J. Teh, “Surveys on the reliability impacts of power system cyber – physical layers,” Sustain. Cities Soc., vol. 62, no. November 2019, p. 102384, 2020.

[9] B. Jimada-Ojuolape and J. Teh, “Impact of the Integration of Information and Communication Technology on Power System Reliability: A Review,” IEEE Access, vol. 8, pp. 24600–24615, 2020.

[10] S. Karimi, P. Musilek, and A. M. Knight, “Dynamic thermal rating of transmission lines: A review,” Renew. Sustain. Energy Rev., vol. 91, no. August 2016, pp. 600–612, 2018.

[11] J. Teh, C. Lai, and Y. Cheng, “Impact of the Real-Time Thermal Loading on the Bulk Electric System Reliability,” IEEE Trans. Reliab., vol. 66, no. 4, pp. 1–10, 2017.

[12] J. Teh and C. M. Lai, “Reliability Impacts of the Dynamic Thermal Rating System on Smart Grids Considering Wireless Communications,” IEEE Access, vol. 7, pp. 41625–41635, 2019.

[13] J. Teh and I. Cotton, “Reliability Impact of Dynamic Thermal Rating System in Wind Power Integrated Network,” IEEE Trans. Reliab., vol. 65, no. 2, pp. 1081–1089, 2016.

[14] S. Almasabi and J. Mitra, “Multistage Optimal PMU Placement Considering Substation Infrastructure,” IEEE Trans. Ind. Appl., vol. 54, no. 6, pp. 6519–6528, 2018.

[15] B. Ramachandran and G. T. Bellarmine, “Improving observability using optimal placement of phasor measurement units,” Int. J. Electr. POWER ENERGY Syst., vol. 56, pp. 55–63, 2014.

[16] Q. Li et al., “An Information-Theoretic Approach to PMU Placement in Electric Power Systems,” IEEE Trans. Smart Grid, vol. 4, no. 1, pp. 446–456, 2013.

[17] B. K. Saha Roy, A. K. Sinha, and A. K. Pradhan, “An optimal PMU placement technique for power system observability,” International Journal of Electrical Power and Energy Systems, vol. 42, no. 1. pp. 71–77, 2012.

[18] A. G. Phadke, “Synchronized phasor measurements in power systems,” IEEE Comput. Appl. Power, vol. 6, no. 2, pp. 10–15, Apr. 1993.

[19] F. Aminifar, M. Fotuhi-Firuzabad, M. Shahidehpour, and A. Safdarian, “Impact of WAMS malfunction on power system reliability assessment,” IEEE Trans. Smart Grid, vol. 3, no. 3, pp. 1302–1309, 2012.

[20] J. Teh, “Uncertainty Analysis of Transmission Line End-of-Life Failure Model for Bulk Electric System Reliability Studies,” IEEE Trans. Reliab., vol. 67, no. 3, pp. 1261–1268, 2018.

[21] J. Teh et al., “Prospects of Using the Dynamic Thermal Rating System for Reliable Electrical Networks: A Review,” IEEE Access, vol. 6, pp. 26765–26778, 2018.

[22] F. Massaro, M. G. Ippolito, E. M. Carlini, and F. Bassi, “Maximizing energy transfer and RES integration using dynamic thermal rating: Italian TSO experience,” Electr. Power Syst. Res., vol. 174, no. April, p. 105864, 2019.

[23] S. S. Mousavi-Seyedi, F. Aminifar, S. Azimi, and Z. Garoosi, “On-line assessment of transmission line thermal rating using PMU data,” Smart Grid Conf. 2014, SGC 2014, pp. 1–6, 2014.

[24] R. K. Mai, L. Fu, and Xu HaiBo, “Dynamic line rating estimator with synchronized phasor measurement,” APAP 2011 - Proc. 2011 Int. Conf. Adv. Power Syst. Autom. Prot., vol. 2, pp. 940–945, 2011.

[25] M. K. Metwaly and J. Teh, “Fuzzy Dynamic Thermal Rating System based SIPS for Enhancing Transmission Line Security,” IEEE Access, vol. 9, pp. 1–1, 2021.

[26] A. G. Phadke and J. S. Thorp, Synchronized Phasor Measurements and Their Applications (Power Electronics and Power Systems). 2008.

[27] Transmission and Distribution Committee of the IEEE Power Engineering Society, IEEE Std 738 - 2006 - Standard for Calculating the Current-Temperature of Bare Overhead Conductors, vol. 2006, no. January. 2007.

[28] Met Office, “MIDAS Open: UK mean wind data, v201908,”

Authorized licensed use limited to: University of Durham. Downloaded on January 06,2022 at 14:00:51 UTC from IEEE Xplore. Restrictions apply.

Centre for Environmental Data Analysis, 2019. [Online]. Available: http://data.ceda.ac.uk/badc/ukmo-midas-open/data/uk-mean-wind-obs/dataset-version-201908/lincolnshire/00405_donna-nook-no-2. [Accessed: 02-Oct-2020].

[29] R. Billinton and L. Wenyuan, Reliability Assessment of Electric Power Systems Using Monte Carlo Methods. Springer Science+Business Media, 1994.

[30] R. Billinton and R. N. Allan, Reliability Evaluation of Power Systems. 1986.

[31] P. F. Albrecht et al., "IEEE reliability test system: A report prepared by the Reliability Test System Task Force of the Application of Probability Methods Subcommittee," IEEE Trans. Power Appar. Syst., vol. PAS-98, no. 6, pp. 2047–2054, 1979.

Authorized licensed use limited to: University of Durham. Downloaded on January 06,2022 at 14:00:51 UTC from IEEE Xplore. Restrictions apply.